International Journal of Nanomedicine

Dovepress
open access to scientific and medical research

Open Access Full Text Article

ORIGINAL RESEARCH

Preparation of Ag Nanoclusters-Modified Non-Sintered Silica Ceramic-Like Nanosheet for Removing Dyes and Bacteria from Water

This article was published in the following Dove Press journal:
International Journal of Nanomedicine

Xiuli Ren[1]
Xinyan Lv[1]
Zhenhua Chen[1]
Peng Zhang[1]
Xun Hu Snr[2]
Xifan Mei[1]

[1]Jinzhou Medical University, Jinzhou, 121001, Liaoning, People's Republic of China; [2]University of Jinan, Jinan, 250022, Shandong, People's Republic of China

Purpose: Worldwide water contamination treatment and water security are essential for all living organisms. Among various water contaminants, dye, and bacteria pollution needs to be solved urgently.

Methods and Results: In this work, a ceramic sheet from monodisperse, porous silica nanospheres (SiO_2 NSs) with an average diameter of 220 was prepared. The prepared SiO_2 ceramic sheets were investigated as a "filtration" material in removing dyes (alcian blue, AB; and methylene blue, MB) and bacteria (*E. coli and S. aureus*). The obtained sheets had efficient adsorption efficiency of 98.72% (for AB) and 97.35% (for MB), and a high adsorption capacity for AB is 220 (mg/g), for MB is 176 (mg/g). Furthermore, these SiO_2 ceramic sheets had a high recycling capability for removing dyes by calcination. Being modified by Ag nanoclusters, the ceramic sheets present a strong bactericidal function.

Conclusion: Our results demonstrated that the obtained SiO_2 non-sintered ceramic sheets is rapid and efficient in the filtration of dyes and bacteria from polluted water.

Keywords: SiO_2 nanospheres, ceramic sheet, Ag nanoclusters, water treatment

Introduction

Water pollution is a significant challenge to people's health. Among various water contaminates, dye and bacteria pollution needs to be solved urgently.[1] Wastewater discharged from the textile, printing, and dyeing industries causes serious problems for the environment and human life.[1–3] Among these toxic pollutants, dyes are non-degradable and toxic, and the presence of even a low concentration in water is visible and highly undesirable.[4,5] Meanwhile, dyes are resistant to degradation because of their stable chemical structure.[6] In addition to dye pollution, bacterial infection remains one of the leading causes of death worldwide.[1] Thus, to ensure water security, removing dyes and bacterial from polluted water is the essential problem to solve.

The conventional ways to treat dye polluted water consist of extraction, flocculation, precipitation, photo-catalytic degradation and biological oxidation.[7–10] However, these methods may have the disadvantages of being time-consuming, difficult in their operation, low in efficiency, and have inconvenient treatment effects.[11] Compared with other methods, adsorption methods are easy in their operation, are highly efficienct, and low in cost, and have been widely used for removing toxic dye from discharged water.[12,13] Currently, various types of

Correspondence: Zhenhua Chen; Xifan Mei
Email zhchen561@yahoo.com; meixifan1971@163.com

submit your manuscript | www.dovepress.com
DovePress
http://doi.org/10.2147/IJN.S286406

functional materials including activated carbon, graphene oxide, nanomaterials and polymeric composites have been widely developed for water treatment.[14–23] However, some properties, such as high efficiency, easy operation, and recyclability, are still challenges for removing materials for dyes.[24] Recently, nanomaterials are being widely used in removing dye from wastewater because of their unique properties.[25] Among them, silica nanospheres have been extensively used because of their non-toxic, high porosity surface.[26,27] In the present work, porous SiO_2 NSs were prepared by a simple method. Considering porous SiO_2 NSs powders used for dye adsorption involving multiple processes including centrifugation, drying, and collection. These processes reduce the adsorption efficiency and are not conducive to practical application. And, based on the technology of geologically-inspired strong bulk ceramics,[28] we made these obtained SiO_2 NSs powders into a highly dense ceramic-like material. The motivation to design the novel ceramic material is: 1) The use of bulk ceramic materials can be a simpler and more effective filtration method to treat sewage, instead of centrifugation or long-term sedimentation like nanomaterials; and 2) dense bulk materials can reduce the leakage of nanoparticles and reduce their potential toxicity. The prepared SiO_2-ceramic material was used as a filter, it possesses the advantages of fast adsorption, high adsorption capacity, and recyclability. It has been reported that composites modified with Ag nanoparticles can effectively reduce the leakage of free silver nanoparticles to reduce potential toxicity, while having a good bactericidal effect.[18,29–31] Therefore, we proposed the removing of dyes and bacteria from water using Ag nanoclusters (NCs) decorated SiO_2 sheet (ANSS) as illustrated in Scheme 1.

Experimental

Materials

NH_3 solution (28 wt%), $AgNO_3$, and ethanol were obtained from Tianli Chemical Reagent Co., Ltd, China. TP (Green tea polyphenols) (≥ 98 wt%, Wuxi Taiyo Green Power Co. Ltd., Jiangsu, China). Tetraethyl orthosilicate (AR) and NaOH (GR) was obtained from Tianli Chemical Reagent Co., Ltd, China. AB, MB and poly(vinylpyrrolidinone) (PVP) (30 000MW) were obtained from Sigma (St. Louis, MO, USA). All the experiments used deionized water. AB is a stain for connective tissue mucins and a number of epithelial mucins and as a gelling agent for lubricating fluids. MB is an organic dye of the thiazine group, used in medicine as an antiseptic and as an antidote for certain types of poisoning.

Preparation of Silica Porous NSs

The preparation of silica porous NSs is according to the previous work.[32] The procedure is as follows: ethanol-water co-solvent system was chosen, briefly, 1.8 mL of ammonia solution, 2.48 mL of ethanol and 1.0 mL of H_2O were mixed together in a 20 mL erlenmeyer flask. The mixture was stirred (1000 rpm, magnetic stirrer) for 8 minutes. Then, 0.2 mL of TEOS was rapidly added to the flask. After 30 seconds, the stirring speed was adjusted to 500 rpm.

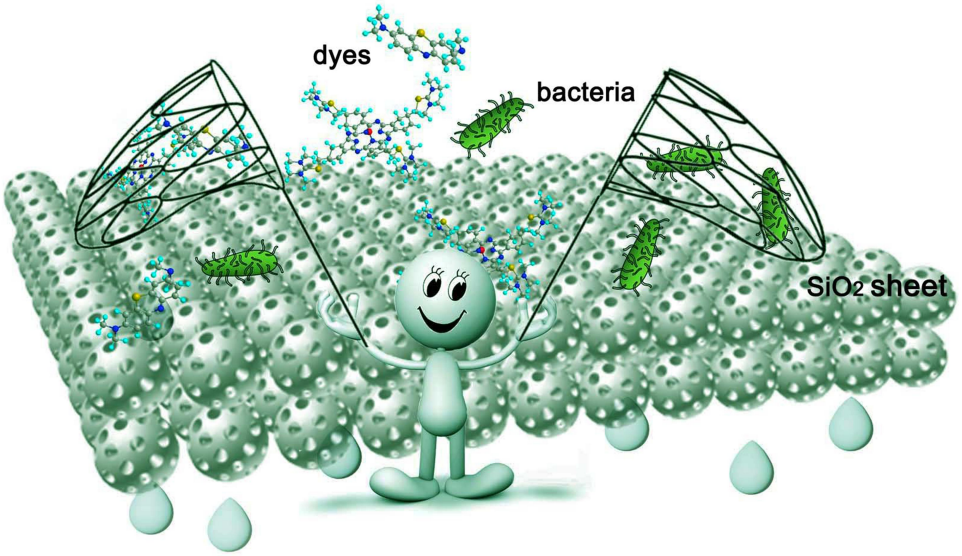

Scheme 1 Illustration of removing dyes and bacteria by using nano silicon dioxide sheet.

After that, the experiment was further reacted for 1.5 hours. The products were collected by centrifugation and rinsed by deionized water several times. After that, 0.03 g lyophilized silica nanospheres were dispersed in 5 mL H_2O with the aid of ultrasonication. After being treated for 24 h, the obtained nanospheres were centrifuged (10,000 rpm, 5 min), and rinsed thoroughly by water and ethanol. Finally, the obtained silica nanospheres were freeze dried.

Preparation of Ag NCs Modified SiO_2 NSs

0.05g TP was added into 100 mL H_2O under stirring to dissolve. Subsequently, 0.05g lyophilized SiO_2 NSs were dispersed in the TP solution with ultrasonic for 15 minutes. After that, the mixture was placed still on the bench for 3 hours. Then, TP adsorbed SiO_2 NSs was rinsed by water and collected by centrifugation for further use. 0.05g TP adsorbed SiO_2 NSs and 0.01g PVP was added into 100 mL deionized water, stirring for 1 hour. Then, $AgNO_3$ (3 mL, 2 mM) was added into the above mixture at 80°C drop by drop. After reacted at 80°C for 3 hours, the mixture was centrifuged and rinsed by water and ethanol alternatively. Finally, the obtained Ag NCs modified SiO_2 NSs were lyophilized for further use.

Preparation of SiO_2 Sheet

The detailed preparation process of the SiO_2 sheet was illustrated in Figure 1F. Briefly, 0.3g SiO_2 NSs lyophilized powder and 0.06g water were added into the mortar and mixed well. Then, the mixture was put into the mold of the infrared tablet press with a diameter of 13mm. The mold was put into the tablet press and pressed with appropriate pressure. The constant pressure was maintained for 10 minutes, and then the SiO_2 sheet is ready.

Preparation of Ag NCs Decorated SiO_2 Sheet (ANSS)

The process steps are similar to the SiO_2 sheet. Ag NCs decorated SiO_2 NSs were used as building blocks to get ANSS instead of SiO_2 NSs.

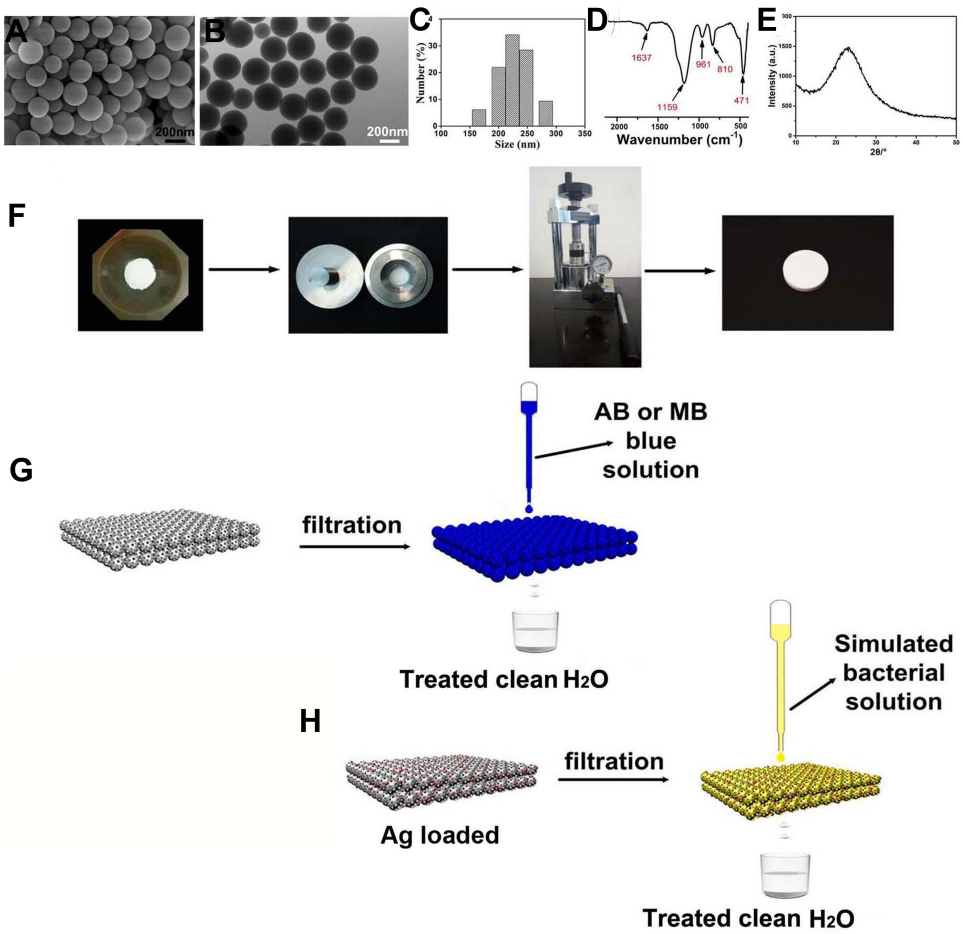

Figure 1 Characterization of the obtained SiO_2 nanospheres: (**A**) SEM image; (**B**) TEM image; (**C**) DLS result; (**D**) FTIR spectrum; (**E**) XRD reflection. (**F**) the schematic preparation of SiO_2-ceramic sheet by non-sintered pressure method. (**G** and **H**) the schematic filtration of dye- and bacteria-polluted water, respectively.

Characterization

The morphology of the porous SiO_2 NSs, Ag NCs decorated SiO_2 NSs, SiO_2 sheet and Ag NCs decorated SiO_2 sheet (ANSS) were investigated by scanning electron microscopy (SEM, Hitachi, S4800), and transmission electron microscopy (TEM, Tecnai G2, 200 kV). Size distribution of the obtained porous SiO_2 NSs was measured by DLS (dynamic Light Scattering, Malvern, Nano ZS90). The composition of the samples was confirmed by FT-IR (Optical Instrument Co., Ltd. Tianjin, China). Crystallographic information of the products was collected by XRD (SHIMADZU, Kyoto, Japan). BET (Brunauer-Emmet-Teller) and BJH (Barrett-Joyner-Halenda) were carried out to analyze the surface area and pore size distribution of the samples. TGA (thermogravimetric data) of the products were performed on NETZSCH STA 449C. UV-vis were carried on PerkinElmer Lambda 605S. CLSM (Confocal laser scanning microscopy; Leica TSC SP5) was adopted to record cell morphology information.

Dyes Filtration

Two cationic dyes (AB, MB) were chosen, their chemical formulae were listed in Figure 2. Firstly, solution of 0.4 mmol/L AB and 1.2 mmol/L MB were prepared before filtration. The adsorption capacity (q_e) and removal efficiency (D) during the filtration were calculated by following equations.[32]

$$q_e(\mathrm{mg/g}) = \frac{(C_0 - C_e)V}{W} \quad (1)$$

$$\mathrm{D} = \frac{A_0 - \mathrm{A}}{A_0} \times 100\% \quad (2)$$

Where C_0, C_e are the initial and the equilibrium dye concentrations (mg/L), V is the volume (L), and W is weight of the adsorbent (g). Where A_0 and A are the absorbance of dye solutions before and after filtration.

Antibacterial and Cell Experiment

Staphylococcus aureus (S. aureus) and Escherichia coli (E. coli) were chosen as the bacterial model. *S. aureus* and *E. coli* were cultured at 37 °C with and without ANSS for given time, respectively. Then, they were measured at 600 nm by spectrophotometer (Hitachi U-3010). Meanwhile, *S. aureus* and *E. coli* solutions grown to appropriate concentrations were used for antibacterial filtration experiments.

Pre-osteoblasts (MC3T3-E1) was used as model cell. MTT assay was performed to investigate the cell viability of MC3T3-E1 cultured with SiO_2 sheet and ANSS at various time. CLSM images were carried out when investigating cells cultured with ANSS and in the control group, respectively.

All the experiments were carried out in triplicate.

Results and Discussion

SEM image (Figure 1A) revealed the spherical shape of the SiO_2 products. TEM image (Figure 1B) further indicated monodispersed property of these prepared SiO_2 NSs. The size distribution result (Figure 1C) indicates that these SiO_2 NSs have an average diameter of 220 nm. HRTEM image (Figure S1A) reveals that the classical SiO_2 NS is covered with a porous surfaces. BET result (Figure S1B) reveals that those porous SiO_2 NSs having a surface area of 346 m^2/g.

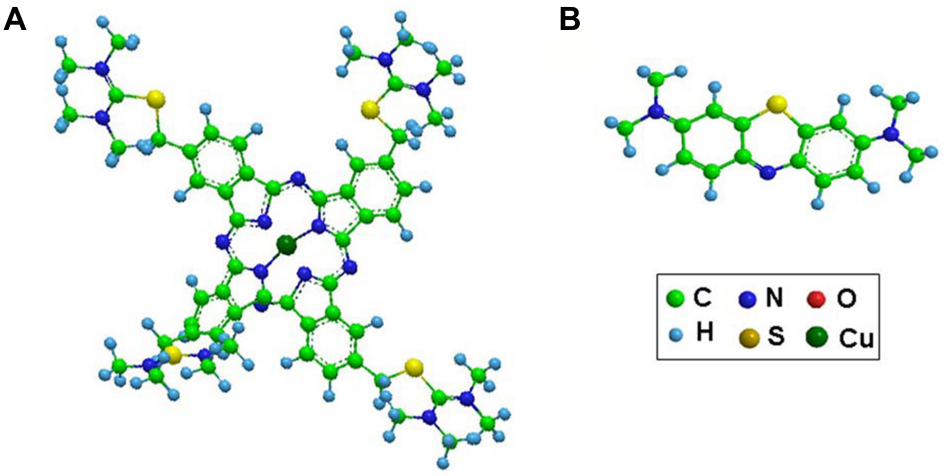

Figure 2 Chemical structure of (**A**) AB; (**B**) MB.

Figure S1C proves that these nanospheres have pores with an average size of ~1.7 nm according to BJH data. FT-IR spectra (Figure 1D) of these nanospheres indicate that the adsorptions at 471, 810, 1159 cm^{-1} belong to Si-O-Si bending.[25] And the adsorption at 961 cm^{-1} belong to Si-OH. The absorption at 1637 cm^{-1} might be due to the hydrogen bond of surface adsorbed water from the surrounding. XRD Broad diffraction at 2θ =23° (Figure 1E) confirms amorphous SiO_2 exist. Figure 1F proves that the SiO_2 sheet can be prepared by infrared tablet press from lyophilized SiO_2 NSs powder. The obtained SiO_2 sheet and ANSS could be used for dye and bacterial filtration as illustrated in Figure 1G and H.

To investigate the adsorption ability of the obtained SiO_2 sheet, as illustrated in Figure 2, we chose AB and MB as model dyes. Our previous work has proven that colloidal silica nanospheres are efficient and recyclable in removing dyes.[32] However, the drawbacks of using colloidal nanospheres for removing dyes in water are obvious because of the difficult recovery of nanomaterials after dye adsorption. Long-term sedimentation and other recovery methods such as centrifugation are not suitable for dye adsorption of natural water resources. Thus, in this work, inspired by compaction of geological, natural mineral sediments, we proposed the room temperature way to prepare SiO_2 sheet by pressure forming. Figure 3 clearly reveals the relationship between pressure and product morphology. Figure 3A shows that when the pressure was 4 MPa, the products were some loose small agglomerates, which do not form a whole sheet. SEM image (Figure 3D) further indicates that these agglomerates were composed by numerous SiO_2 NSs. When the pressure was 7 MPa, a wafer-like sheet (Figure 3B) with a thickness of 0.97mm and a diameter of 13mm was obtained. SEM image (Figure 3E) indicates the surface structure of the obtained SiO_2 flake was made up of porous silica nanoparticles closely arranged, most of which had complete morphology. But a few of them were affected by pressure, and their structures have been damaged and fused with each other (arrows indicated in Figure 3E). While the pressure increased to 15MPa, the thickness of the obtained SiO_2 sheet was decreased to 0.68 mm. And SEM image (Figure 3F) indicates the surface structure of the obtained SiO_2 flake was made up of porous silica nanoparticles fused with each other, only a few areas present pore structure (indicated by the arrows in Figure 3F). The relationship between sheet thickness and pressure is shown in Figure 3G. As the pressure increases, the thickness of the sheet

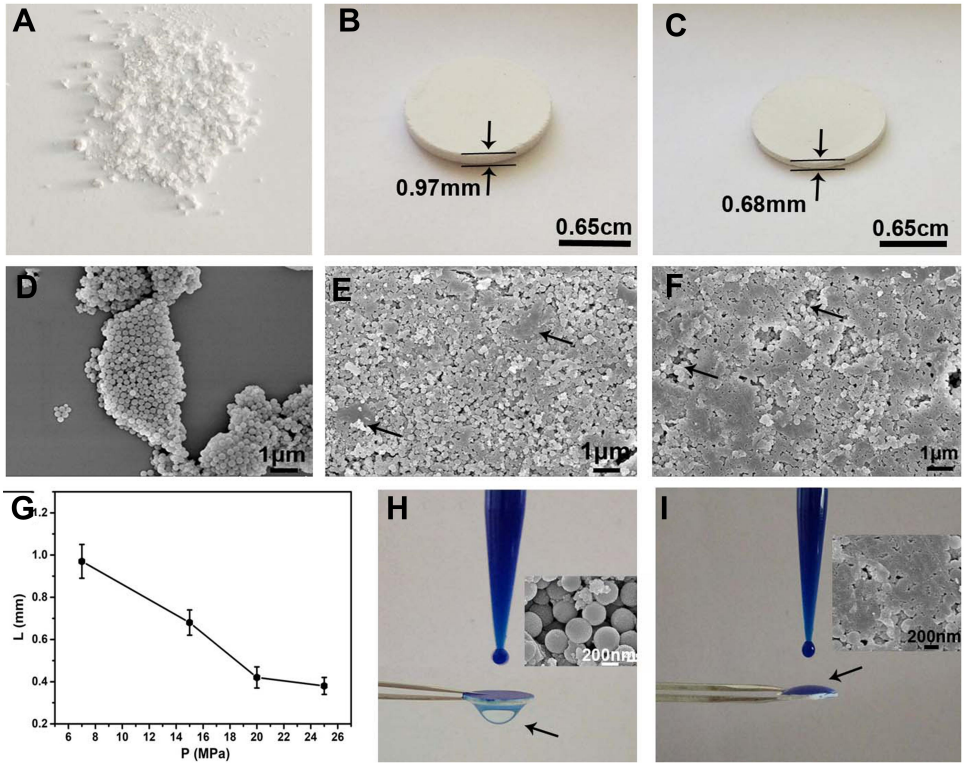

Figure 3 (**A**–**C**) photographs and (**D**–**F**) SEM images of the samples obtained under different pressure: (**A** and **D**) 4MPa; (**B** and **E**) 7MPa; (**C** and **F**) 15MPa. (**G**) relationship between sheet thickness and applied pressure. (**H** and **I**) photographs of methylene blue solution filtered with different SiO_2 sheets, (**H**) used the sheet illustrated in (**B**); (**I**) used the sheet illustrated in (**C**); the inserts are the detailed SEM images of the used SiO_2 sheets, respectively.

gradually decreases. This probably suggests that a more condensed and tougher product will be obtained at higher pressure. Figure 3H reveals that SiO_2 sheet obtained at 7 MPa with porous structure could efficiently filtrate methylene blue solution quickly. However, Figure 3I shows that the SiO_2 sheet obtained at 15 MPa with a condensed structure was disabled in filtrating methylene blue solution. The dye drops were stacked on the sheet and difficult to filter. These results suggest that in order to maintain good filtration performance, a certain degree of compactness must be sacrificed.

The detailed fast filtration process of methylene blue solution by SiO_2 sheet prepared under 7MPa is illustrated in Figure 4; it took only 2.3 seconds to complete the filtration of 0.6 mL dye solution from the beginning of the drips onto the filter sheet. A full video description is provided in the supporting information (Supplementary video). The insert in the last image of Figure 4 indicates that the color contrast between the dye liquid and the filtered liquid is clear, showing that the prepared filter has a good filtering effect.

The stability of the samples was investigated by employing XRD and Raman to test the sample collected after the adsorption experiment. In Figure S2, compared with pure SiO_2, the XRD of SiO_2 after adsorbing dyes has little difference. The slight difference may be that the dispersion peak at 2θ=22.8 in the sample after adsorbing the dye seems to increase in width compared to pure SiO_2. This may be due to the adsorption of the dye further weakening the diffraction signal of some very fine crystalline nanoparticles in the SiO_2 sample.[33] This speculation is further confirmed by Raman spectroscopy data. This speculation is further confirmed by Raman spectra. In Figure S3, the intensities of the Raman scattering peaks of SiO_2 at 470–524cm^{-1}, 1312cm^{-1}, and 1592cm^{-1} (Si-O band) were all weakened after the dye was adsorbed. This may be because the scattering signal of some very fine crystalline nanoparticles in the SiO_2 sample was weakened due to the adsorption of dye. It can also be seen from Figure S3 that the Raman scattering peaks at 972cm^{-1}, 2912cm^{-1}, 2976cm^{-1} (O-H band[34]) in pure SiO_2 were significantly weakened after the dye was adsorbed.

To investigate the filtration ability of SiO_2 sheet, we used the SiO_2 sheet to filter AB and MB solutions (5 mL). As showed in Figure 5A and B, after filtration, characteristic absorption peaks of AB and MB almost disappeared in filtration. These data suggest that SiO_2 sheet was highly

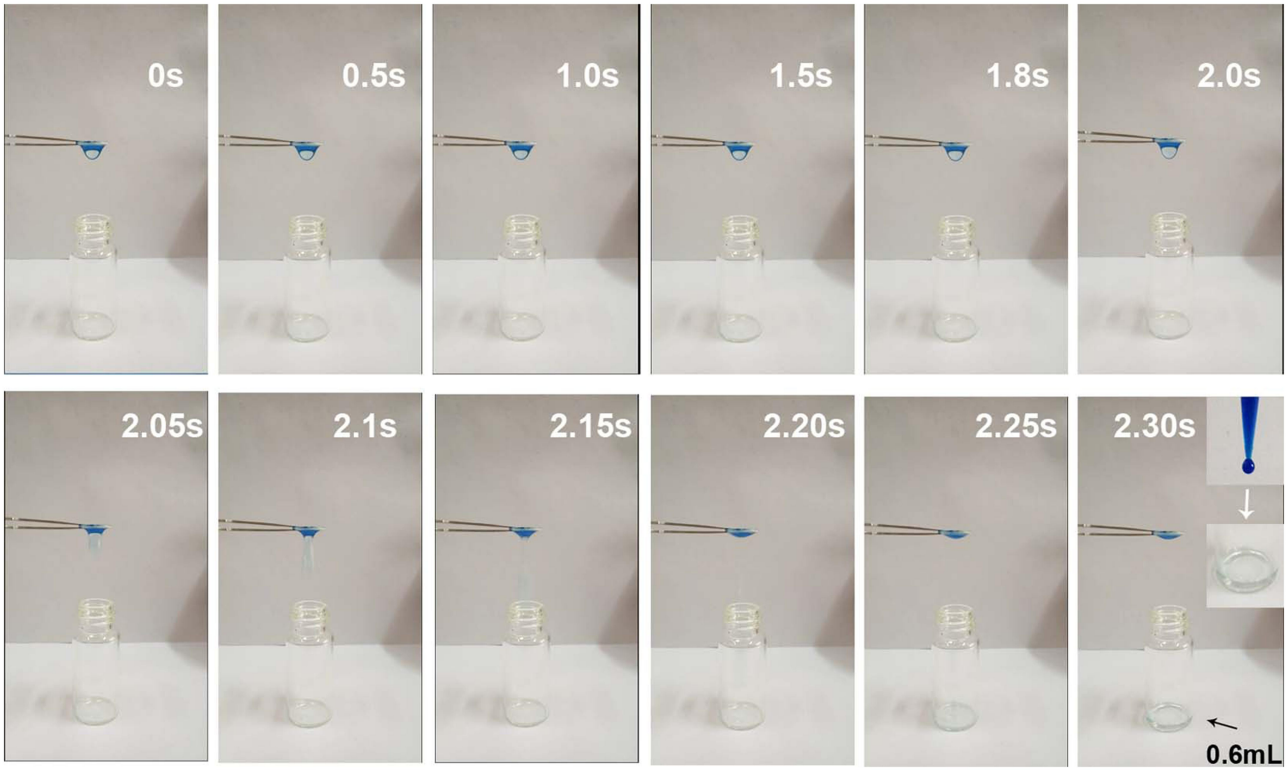

Figure 4 The detailed filtration process of methylene blue solution with SiO_2 sheet prepared under 7 MPa. The full filtered video was provided in the supporting information.

efficient in adsorption dyes. The calculated adsorption efficiencies are 98.72% for AB and 97.35% for MB, respectively. The calibration curve method was used to research adsorption capacity of the SiO_2 sheet according to the method reported previously.[32,35,36] 3×10^{-3} mol/L AB solution and 9 $\times10^{-3}$ mol/L MB solutions were prepared. The obtained calibration curves fit the following equations:

$$A = 277.40038 \times C + 0.00607 \quad (3)$$

$$A = 629.09241 \times C + 0.01783 \quad (4)$$

A is absorbance, C is concentration (mmol/L). Equations (3) is for AB, (4) is for MB. Calculated data suggest these SiO_2 sheets having maximum adsorption capacities of 220 mg/g for AB, and 176×10^{-3} mg/g for MB.

The recyclability of the SiO_2 sheet was tested 6 cycles (adsorption and desorption). Results are shown in Figure 5C and D. Figure 5C presents the color change before adsorption, adsorption, and after desorption. Figure 5D further revealed that, in the first run, the removal efficiency is 98.72% for AB and 97.35% for MB. Moreover, it was found that efficiency was 96.56% for AB and 95.15% for MB after the sixth cycle. These data proved that the SiO_2 sheet has good recyclability. Thermogravimetric analysis (TGA, Figure 5E–G) proved the filtration ability of these SiO_2 sheets. Tiny weight loss of 3.35% (Figure 5E) may be because of the adsorbed H_2O. During the filtration process, SiO_2 sheet has adsorbed amounts of 26.99 weight % for AB (Figure

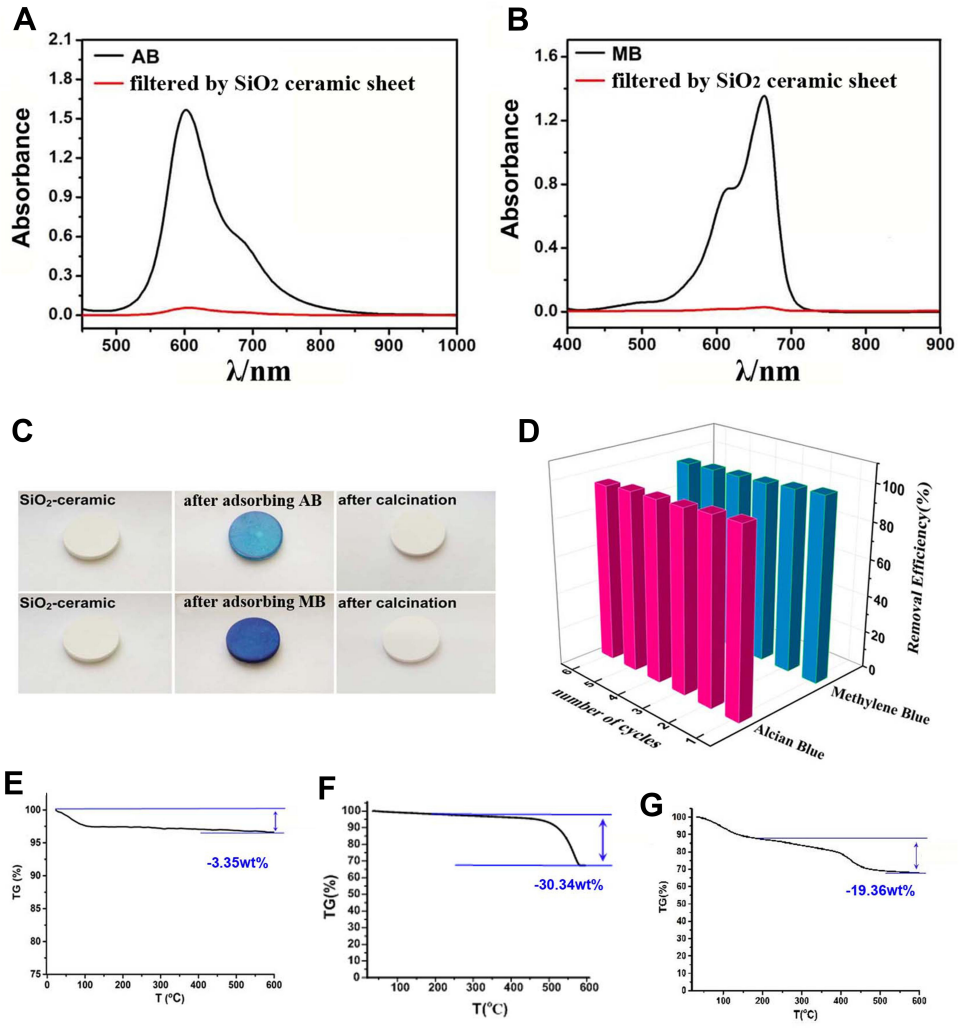

Figure 5 Absorbance spectra of AB solution (**A**) and MB solution (**B**). (**C**) photographs of filtration and sintering recycling process of using SiO_2 sheet to remove AB and MB from water. (**D**) recyclability results. Thermogravimetric curves for (**E**) SiO_2 sheet; (**F**) SiO_2 sheet saturated with AB dyes; (**G**) SiO_2 sheet saturated with MB dyes.

5F) and 16.01 weight % for MB (Figure 5G), respectively. The difference in adsorption weight shown by the TGA data is due to the different molecular weights of AB and MB. The dye removal mechanism of the SiO_2 sheet for AB and MB is contributed by the electrostatic interaction between the cationic dye molecules and anion porous silica nanospheres. Previous zeta potential distribution research found that: SiO_2 NSs presents negatively

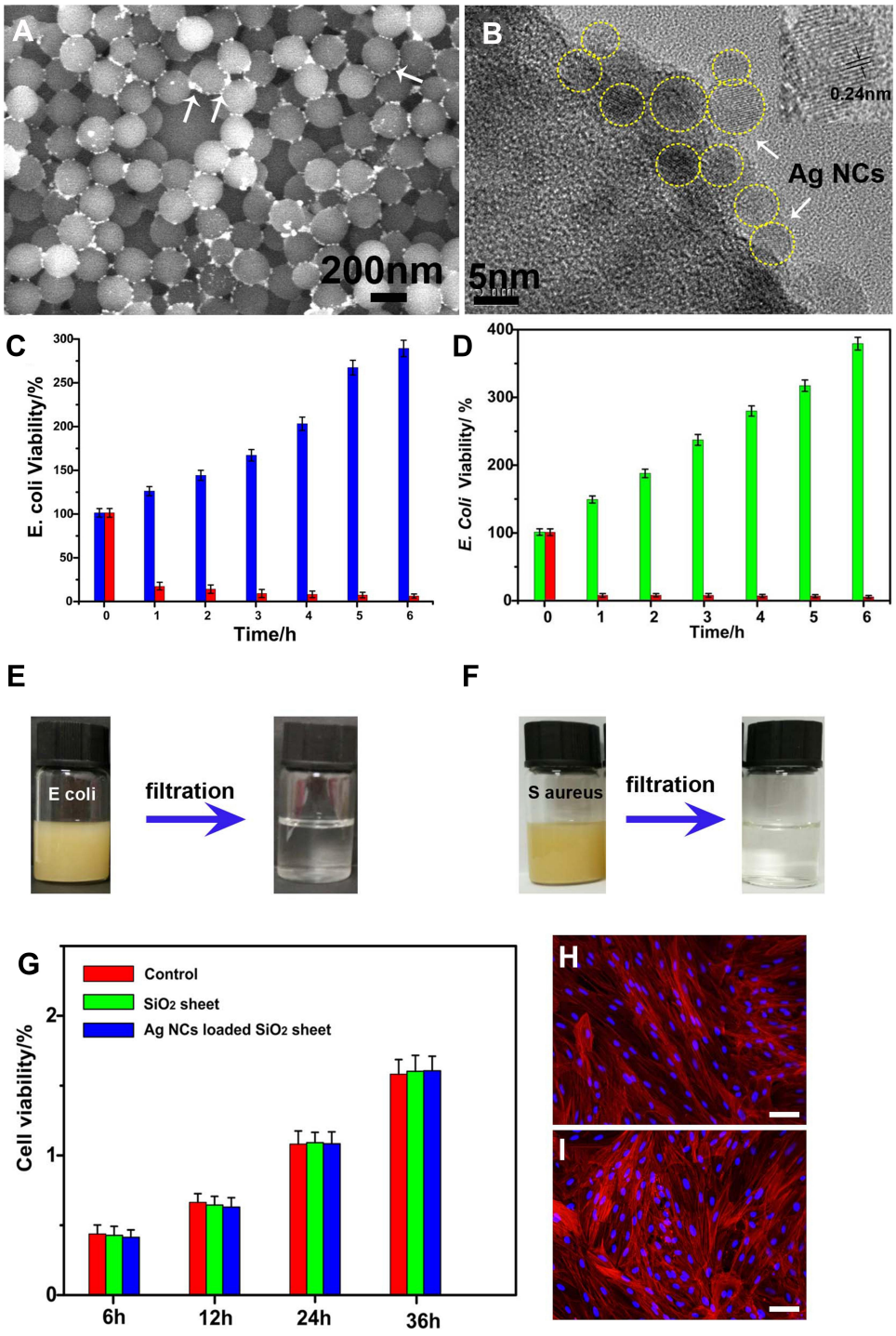

Figure 6 (**A**) SEM image SiO_2 nanospheres coated by Ag nanoclusters (indicated by the arrows); (**B**) HRTEM image of single classical Ag coated SiO_2 nanosphere, the insert indicates 0.25nm lattice phase of Ag nanocluster; time-dependent viability (calculated by turbidity at 600 nm) of E. coli (**C**) and S. aureus (**D**) with and without Ag@SiO_2 sheet. Photographs of E. coli (**E**) and S. aureus (**F**) solution before and after filtration by Ag@SiO_2 sheet, respectively. (**G**) MC3T3-E1 cell viability cultured with SiO_2 sheet and Ag@SiO_2 sheet extract solution at various time. (**H** and **I**) CLSM images of MC3T3-E1 cells cultured for 36h with Ag@SiO_2 sheet (**H**) and in the control group (**I**).

charged surface (−46.6 mV); while after adsorbing cationic dyes of AB and MB, the surface charges were increased up to about −25 mV. These changes might because the adsorbed positively charged dye molecules had neutralized the surface negative charge on those porous silica nanospheres.[32]

The morphology of the prepared Ag NCs modified SiO_2 NSs was shown in Figure 6A, as the arrows indicated, small Ag nanoclusters were found adhered on those SiO_2 nanospheres. HRTEM image (Figure 6B) revealed distribution details of Ag NCs on SiO_2 sphere. The insert in Figure 6B further confirmed the lattice phase of 0.25 nm for Ag NCs, which corresponds to the {111} reflection.[37] The obtained SiO_2 NSs adhered by Ag NCs could effectively reduce the release of free Ag nanoparticles to decrease the potential toxicity, while having a good bactericidal effect. This kind of strategy of fixing Ag nanoparticles by forming composites was inspired by the reported works.[29–31] The antibacterial performance of Ag NCs decorated SiO_2 sheet (ANSS) was illustrated in Figure 6C and D. From these data, it is clear that ANSS can effectively inhibit the proliferation of Escherichia coli and Staphylococcus aureus. Figure 6E and F show comparison pictures of the bacterial solution before and after filtration. As can be seen from the photos, ANSS has a good filtering and sterilizing effect. The antibacterial mechanism of the Ag@SiO2 sheet is that after the bacteria Ag@SiO2 sheet is filtered, it will produce Ag ions and active oxygen in contact with the nano-Ag, thereby killing the bacteria.

To verify the biocompatibility of ANSS, normal cell (MC3T3-E1) culture experiments were performed using the extract of ANSS, and the results are shown in Figure 6G. The data in Figure 6G shows that unlike blank control, pure SiO2 group, ANSS does not show cytotoxicity and has good cell compatibility. CLSM images of MC3T3-E1 cells cultured for 36 h with ANSS extract (Figure 6H) further confirm that the normal spindle cell morphology is almost the same as that shown in Figure 6I.

Conclusion

In summary, inspired by natural geological compacted mineral, we proposed a simple method to prepare SiO_2 ceramic-like sheet by pressure forming at room temperature. The obtained sheets had efficient adsorption efficiency of 98.72% (for AB) and 97.35% (for MB), and high adsorption capacity for AB is 220 (mg/g), for MB is 176 (mg/g). Furthermore, these SiO_2 ceramic sheets had a high recycling capability for removing dyes by calcination. Being modified by Ag nanoclusters, the ceramic sheets present a strong bactericidal function. These data suggested that the SiO_2 ceramic sheets could be applied as a rapid, efficient, and recyclable filtration material for removing dyes and bacteria from polluted water. The prepared ceramic sheet formed by monodisperse porous silica nanospheres adhered with Ag nanoclusters. The strategy of fixing Ag nanoparticles on SiO_2 ceramic-like sheet would effectively reduce the release of free Ag nanoparticles to decrease the potential toxicity, and avoid the drawbacks of long-term sedimentation and other recovery methods for colloidal nanospheres after dye treatment.

Acknowledgments

This work was funded by the National Natural Science Foundation of China (No. 81771987, 82072076), and the Young Top Talents in Xing Liao Talents Program of Liaoning Province (XLYC1807183).

Disclosure

The authors declare no conflict of interest.

References

1. Tomei MC, Pascual JS, Angelucc DM. Analysing performance of real textile wastewater bio-decolourization under different reaction environments. *J Clean Prod*. 2016;129:468–477. doi:10.1016/j.jclepro.2016.04.028
2. Luan MM, Jing GL, Piao YJ, Liu DB, Jin LF. Treatment of refractory organic pollutants in industrial wastewater by wet air oxidation. *Arab J Chem*. 2017;10:769–776. doi:10.1016/j.arabjc.2012.12.003
3. Rajoriya S, Bargole S, George S, Saharan VK. Treatment of textile dyeing industry effluent using hydrodynamic cavitation in combination with advanced oxidation reagents. *J Hazard Mater*. 2018;344:1109–1115. doi:10.1016/j.jhazmat.2017.12.005
4. Liang JY, Ning XA, Kong MY, et al. Elimination and ecotoxicity evaluation of phthalic acid esters from textile-dyeing wastewater. *Environ Pollut*. 2017;231:115–122. doi:10.1016/j.envpol.2017.08.006
5. Reddy CN, Kumar AN, Mohan SV. Metabolic phasing of anoxic-PDBR for high rate treatment of azo dye wastewater. *J Hazard Mater*. 2018;343:49–58. doi:10.1016/j.jhazmat.2017.08.065
6. Bayramoglu G, Akbulut A, Liman G, Arica MY. Removal of metal complexed azo dyes from aqueous solution using tris(2-aminoethyl) amine ligand modified magnetic p(GMA-EGDMA) cationic resin: adsorption, isotherm and kinetic studies. *Chem Eng Res Des*. 2017;124:85–97. doi:10.1016/j.cherd.2017.06.005
7. Hu HS, Yang MD, Dang J. Treatment of strong acid dye wastewater by solvent extraction. *Sep Purif Technol*. 2005;42:129–136. doi:10.1016/j.seppur.2004.07.002
8. Yang ZL, Liu XX, Gao BY, et al. Flocculation kinetics and floc characteristics of dye wastewater by polyferric chloride–polyepichlorohydrin–dimethylamine composite flocculant. *Sep Purif Technol*. 2013;118:583–590. doi:10.1016/j.seppur.2013.08.004
9. Lin WC, Chen CH, Tang HY, et al. Electrochemical photocatalytic degradation of dye solution with a TiO2-coated stainless steel electrode prepared by electrophoretic deposition. *Appl Catal B*. 2013;140:32–41. doi:10.1016/j.apcatb.2013.03.032
10. Li Y, Shi JQ, Qu RJ, et al. Toxicity assessment on three direct dyes (D-BLL, D-GLN, D-3RNL) using oxidative stress bioassay and quantum parameter calculation. *Ecotoxicol Environ Saf*. 2012;86:132–140. doi:10.1016/j.ecoenv.2012.09.023

11. Bhatt AS, Sakaria PL, Vasudevan M, et al. Adsorption of an anionic dye from aqueous medium by organoclays: equilibrium modeling, kinetic and thermodynamic exploration. *RSC Adv*. 2012;2:8663–8671. doi:10.1039/c2ra20347b
12. Wang XH, Jiang CL, Hou BX, Wang YY, Hao C, Wu JB. Carbon composite lignin-based adsorbents for the adsorption of dyes. *Chemosphere*. 2018;183.
13. Wang YY, Zhu LL, Wang XH, et al. Synthesis of aminated calcium lignosulfonate and its adsorption properties for azo dyes. *J Ind Eng Chem*. 2018;61:321–330. doi:10.1016/j.jiec.2017.12.030
14. Su SL, Rock KL, Yee MW, et al. Microwave-assisted pyrolysis with chemical activation, an innovative method to convert orange peel into activated carbon with improved properties as dye adsorbent. *J Clean Prod*. 2017;162:1376–1387. doi:10.1016/j.jclepro.2017.06.131
15. Chawla S, Uppal H, Yadav M, Bahadur N, Singh N. Zinc peroxide nanomaterial as an adsorbent for removal of Congo red dye from waste water. *Ecotoxicol Environ Saf*. 2017;135:68–74. doi:10.1016/j.ecoenv.2016.09.017
16. Liu JM, Zhu K, Jiao TF, et al. Preparation of graphene oxide-polymer composite hydrogels via thiol-ene photopolymerization as efficient dye adsorbents for wastewater treatment. *Colloids Surf a Physicochem Eng Asp*. 2017;529:668–676. doi:10.1016/j.colsurfa.2017.06.050
17. Verma SK, Jha E, Panda PK, et al. Molecular insights to alkaline based bio-fabrication of silver nanoparticles for inverse cytotoxicity and enhanced antibacterial activity. *Mater Sci Eng C Mater Biol Appl*. 2018;92:807–818. doi:10.1016/j.msec.2018.07.037
18. Verma SK, Jha E, Panda PK, et al. Rapid novel facile biosynthesized silver nanoparticles from bacterial release induce biogenicity and concentration dependent in vivo cytotoxicity with embryonic zebrafish-a mechanistic insight. *Toxicol Sci*. 2018;161:125–138. doi:10.1093/toxsci/kfx204
19. Arun T, Verma SK, Panda PK, et al. Facile synthesized novel hybrid graphene oxide/cobalt ferrite magnetic nanoparticles based surface coating material inhibit bacterial secretion pathway for antibacterial effect. *Mater Sci Eng C Mater Biol Appl*. 2019;104:109932. doi:10.1016/j.msec.2019.109932
20. Verma SK, Jha E, Panda PK, et al. Molecular aspects of core-shell intrinsic defect induced enhanced antibacterial activity of ZnO nanocrystals. *Nanomedicine*. 2018;13:43–68. doi:10.2217/nnm-2017-0237
21. Chinh VD, Hung LX, Di Palma L, Hanh VTH, Vilardi G. Effect of carbon nanotubes and carbon nanotubes/gold nanoparticles composite on the photocatalytic activity of TiO_2 and TiO_2-SiO_2. *Chem Eng Technol*. 2019;42:308–315. doi:10.1002/ceat.201800265
22. Vilardi G, De Caprariis B, Stoller M, Di Palma L, Verdone N. Intensified water denitrification by means of a spinning disk reactor and stirred tank in series: kinetic modelling and computational fluid dynamics. *J Water Process Eng*. 2020;34:101147. doi:10.1016/j.jwpe.2020.101147
23. Chinh VD, Broggi A, Di Palma L, et al. XPS spectra analysis of Ti^{2+}, Ti^{3+} ions and dye photodegradation evaluation of titania-silica mixed oxide nanoparticles. *Journal of Electron Mater*. 2018;47:2215–2224. doi:10.1007/s11664-017-6036-1
24. Wang SM, Li ZH, Lu C. Polyethyleneimine as a novel desorbent for anionic organic dyes on layered double hydroxide surface. *J Colloid Interface Sci*. 2015;458:315–322. doi:10.1016/j.jcis.2015.07.056
25. Kok BT, Vakili M, Horri BA, Phaik EP, Ahmad ZA, Babak S. Adsorption of dyes by nanomaterials: recent developments and adsorption mechanisms. *Sep Purif Technol*. 2015;150:229–242. doi:10.1016/j.seppur.2015.07.009
26. Chen KJ, Fan WJ, Huang CJ, Qiu XQ. Enhanced stability and catalytic activity of bismuth nanoparticles by modified with porous silica. *J Phys Chem Solids*. 2017;110:9–14. doi:10.1016/j.jpcs.2017.05.025
27. Budnyk AP, Cherkasova SO, Damin A. One-pot sol-gel synthesis of porous silica glass with gold nanoparticles. *Mendeleev Commun*. 2017;27:531–534. doi:10.1016/j.mencom.2017.09.035
28. Bouville F, Studart A. Geologically-inspired strong bulk ceramics made with water at room temperature. *Nat Commun*. 2017;8:14655. doi:10.1038/ncomms14655
29. Alvarez PJJ, Chan CK, Elimelech M, Halas NJ, Villagrán D. Emerging opportunities for nanotechnology to enhance water security. *Nat Nanotechnol*. 2018;13:634–641. doi:10.1038/s41565-018-0203-2
30. Faria AF, Liu C, Xie M, et al. Thin-film composite forward osmosis membranes functionalized with graphene oxide-silver nanocomposites for biofouling control. *J Memb Sci*. 2017;525:146–156. doi:10.1016/j.memsci.2016.10.040
31. Li JH, Shao XS, Zhou Q, Li MZ, Zhang QQ. The double effects of silver nanoparticles on the PVDF membrane: surface hydrophilicity and antifouling performance. *Appl Surf Sci*. 2013;265:663–670. doi:10.1016/j.apsusc.2012.11.072
32. Lv X, Zhao M, Chen Z, et al. Prepare porous silica nanospheres for water sustainability: high efficient and recyclable adsorbent for cationic organic dyes. *Colloid Polym Sci*. 2018;296:59–70. doi:10.1007/s00396-017-4224-4
33. Dembski S, Milde M, Dyrba M, Schweizer S, Gellermann C, Klockenbring T. Effect of pH on the synthesis and properties of luminescent SiO_2/calcium phosphate: Eu^{3+} core-shell nanoparticles. *Langmuir*. 2011;27:14025–14032. doi:10.1021/la2021116
34. Galeener FL, Mikkelsen JC. Raman diffusion profilometry: ohin vitreous SiO_2. *Appl Phys Lett*. 1981;38:336–338. doi:10.1063/1.92361
35. Zhao M, Chen Z, Lv X, et al. Preparation of core-shell structured CaCO3 microspheres as rapid and recyclable adsorbent for anionic dyes. *Royal Soc Open Sci*. 2017;4:170697. doi:10.1098/rsos.170697
36. Chen ZH, Wang CH, Chen JZ, Li XD. Biocompatible, functional spheres based on oxidative coupling assembly of green tea polyphenols. *J Am Chem Soc*. 2013;135:4179–4182. doi:10.1021/ja311374b
37. Zhang M, Zhao A, Guo H, et al. Green synthesis of rosettelike silver nanocrystals with textured surface topography and highly efficient SERS performances. *CrystEngComm*. 2011;13:5709–5717. doi:10.1039/c1ce05105a